

Macroscopic effects of microscopic roughness in suspensions

Helen J. WILSON

Tel.: ++44 (0)20 7679 1302; Fax: ++44 (0)20 7383 5519; Email: helen.wilson@ucl.ac.uk
Mathematics Department, University College London, UK

Abstract We study a model suspension consisting of a monolayer of identical spheres in a viscous medium without Brownian effects. In the absence of inertia, and under the influence of finite forces, perfectly smooth spheres will never come into contact because of the strength of the lubrication interaction. Indeed, an interaction between two spheres is perfectly reversible. However, this ideal is not achieved in practice: careful experiments with just two spheres show that some irreversible interaction occurs. We treat this interaction as a simple contact between the spheres: we assume that they are microscopically rough and have surface asperities which are too sparse to affect the hydrodynamics of the system, but which prevent the particles from approaching beyond some nominal surface separation.

For a dilute suspensions in steady shear flow, a calculation to order c^2 in the particle area concentration shows that roughness actually *lowers* the viscosity of the suspension relative to its value for smooth spheres; this is because the excluded parts of configuration space are those with very close particles, where the lubrication layers cause high dissipation. Negative normal stress differences are also introduced by the roughness.

At higher concentrations we use Stokesian Dynamics to simulate the suspension dynamics. We find that roughness increases the viscosity above an area concentration of around 40% and the normal stress differences become very sensitive to particle configuration, and fluctuate strongly with time.

Keywords: Suspensions, Surface Roughness, Rheology, Stokesian Dynamics, Contact

1. Introduction

It is well known that Stokes flow, the zero-inertia limit of Newtonian fluid flow, is reversible: if all the external forces on a flowing system are instantaneously reversed, in this limit the system should exactly reverse its previous motion and return to its initial configuration. Engaging demonstrations of this in simple flow are readily available, (De Moss and Cahill, 2007). However, when particles are present, experimental evidence (Arp and Mason, 1977; Zeng et al., 1996) shows that flow may not, in practice, be reversible.

The cause here is microscopic surface asperities which can cause contact between particles when their nominal (smooth) surfaces are still a small distance apart. This contact is an irreversible effect. As an example, consider two identical spheres lying in the plane of a shearing flow. If their trajectory is such that their closest

approach is close enough for contact to occur, then at the contact point they are pushed apart by the contact; if the shear flow driving the orbits is reversed, the spheres will not return to their original positions but will have moved further apart in the flow-gradient direction.

In this paper we discuss the effects that such contacts have on the overall rheology of an ideal model suspension. The particles are identical spheres of radius a ; there is no inertia and no Brownian motion; the matrix fluid is Newtonian; and the contact is modelled as simply as possible. Our contact model treats the asperities as being sufficiently sparse to have no effect on the hydrodynamics, but simply applying an interparticle force. This force (equal and opposite on the two spheres in contact) is specified in terms of components. The component parallel to the line of centres of the two spheres is sufficient to exactly halt their approach, and

2.1 Pair distribution function

has magnitude F_n . The perpendicular component opposes the shearing motion between the sphere surfaces, and has maximum magnitude νF_n . The contact model has two parameters: the friction coefficient ν and an effective roughness height $h = a\zeta$. This is the surface separation at which the force comes into action.

Much of this work was presented in an earlier paper (Wilson and Davis, 2002); however, that work omitted all calculation of the second normal stress difference N_2 and had additional small quantitative errors in some of the numerical results. These errors and omissions are corrected here.

2. Dilute Suspensions

We consider a monolayer of spheres of area concentration c in an infinite volume of fluid having viscosity μ . The layer undergoes shearing flow (in the plane of the layer) at shear rate $\dot{\gamma}$. Because the true volume fraction is zero, we normalise stresses by the effective volume of the layer (Brady and Bossis, 1985): that is, its area multiplied by a nominal width $2a$. Using this convention, the leading-order correction to the suspension viscosity η is

$$\eta = \mu \left(1 + \frac{5}{3}c \right). \quad (1)$$

This is the equivalent of Einstein's (Einstein, 1906; 1911) well-known three-dimensional viscosity correction $\eta_{3D} = \mu(1 + \frac{5}{2}C)$ for a suspension at volume fraction C .

When we continue this expansion to order c^2 , the result can no longer be represented by a single scalar viscosity. Instead we must calculate the average stress tensor

$$\Sigma_{ij} = 2\mu E_{ij} + \frac{c}{2\pi a^3} \bar{S}_{ij} \quad (2)$$

where E_{ij} is the symmetric part of the background flow gradient tensor and \bar{S}_{ij} is the average stresslet:

$$\bar{S}_{ij} = \int_A S_{ij}(\mathbf{r}) \mathcal{P}(\mathbf{r}) d^2\mathbf{r} \quad (3)$$

where $S_{ij}(\mathbf{r})$ is the stresslet induced by a pair of particles at positions \mathbf{x}_0 , $\mathbf{x}_0 + \mathbf{r}$ and $\mathcal{P}(\mathbf{r})$ is

the probability of finding two particles in that configuration given that our test particle is at \mathbf{x}_0 (scaled such that $\mathcal{P}(\mathbf{r}) \rightarrow 1$ as $|\mathbf{r}| \rightarrow \infty$).

2.1 Pair distribution function

In the absence of Brownian motion, the pair distribution function $\mathcal{P}(\mathbf{r})$ evolves according to a simple advection equation (the Liouville equation):

$$\nabla \cdot [\mathcal{P}\mathbf{V}] = 0 \quad (4)$$

where $\mathbf{V}(\mathbf{r})$ is the velocity of a sphere centred at $\mathbf{x}_0 + \mathbf{r}$ relative to one centred at \mathbf{x}_0 . This equation is first-order, and may be solved using the method of characteristics, which essentially relates \mathcal{P} at one point on a particle's trajectory to its value at any other point on the trajectory. If the trajectory comes from infinity, our imposed boundary condition $\mathcal{P}(\mathbf{r}) \rightarrow 1$ as $|\mathbf{r}| \rightarrow \infty$ is sufficient to specify the distribution function everywhere on the particle path.

In a simple shear flow containing two solid spheres, some initial configurations cause the spheres to perform orbits (Batchelor and Green, 1972): that is, they periodically move around one another such that the trajectories of one relative to another are closed. These trajectories never see the boundary condition at infinity, and so their pair distribution function \mathcal{P} is not defined¹. So for perfectly smooth spheres, we cannot calculate the suspension viscosity to order c^2 . However, the largest of these orbits has a closest approach separation of $2.1 \times 10^{-4}a$, which is lower than many estimates of the size of particle roughness. If the roughness height is larger than this value, then the effect of contact is to break *all* closed trajectories. Particles which would have carried out closed orbits are moved outwards by contact and eventually become well separated. The pair distribution function is now well-defined everywhere, and takes the form illustrated schematically in figure 1. We are defining the x -direction as the flow direction and the y -direction as the flow gradient

¹The inclusion of weak Brownian motion would cause \mathcal{P} to be defined everywhere, but at the expense of the simplicity that allows us to calculate most of the quantities in this paper.

2.2 Stresslet calculation

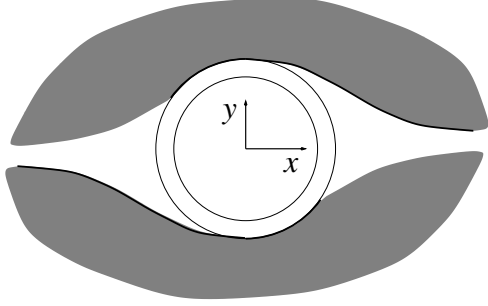


Figure 1: Schematic of the pair distribution function in the case where contact breaks all closed orbits. Particles which would otherwise have been in the white region are on trajectories which come closer than contact. At close approach, they are moved onto the contact surface (high \mathcal{P} , thick-lined portion of the outer circle) which they then leave at $x = 0$ onto a sheet of high \mathcal{P} . Thus the black regions of very high particle density contain all the particles missing from the white regions. Taken from figure 1 of Wilson and Davis (Wilson and Davis, 2002).

direction in this shearing flow.

In the bulk (grey) region, the pair distribution is unaffected by contact, and is given by²

$$\mathcal{P}(\mathbf{r}) = (1 - A(s))^{-1} \phi^{-2}(s) \quad (5)$$

$$\phi(s) = \exp \left[\int_s^\infty \frac{A(s') - B(s')}{1 - A(s')} \frac{ds'}{s'} \right] \quad (6)$$

in which we have defined the scalar separation $s = |\mathbf{r}|/a$, and the functions $A(s)$ and $B(s)$ are two-sphere hydrodynamic functions (Kim & Karrila, 1991).

On the contact surface (black arc), the distribution function must be calculated numerically; and since this provides the upstream boundary condition for the sheet region (black curve) the contribution from the sheet, too, is dependent on one numerically calculated data point.

In the wake (white) region, we have $\mathcal{P} = 0$ so this region does not contribute to the stress integral of equation (3).

²There was a typographical error in the definition of $\phi(s)$ in equation (2.8) of Wilson and Davis (Wilson and Davis, 2002); the form given here is correct.

2.2 Stresslet calculation

There are two possible sources of stresslet for a given configuration of two particles. There is the hydrodynamic stresslet, given by their direct interaction with the fluid:

$$S_{ij}^H = \frac{20}{3} \pi a^3 \mu \left\{ (1 + K(s)) E_{ij} + L(s) (n_i E_{jk} n_k + n_j E_{ik} n_k - \frac{2}{3} n_k E_{kl} n_l \delta_{ij}) + M(s) (n_i n_j - \frac{1}{3} \delta_{ij}) n_k E_{kl} n_l \right\}, \quad (7)$$

and, if the particles are in contact, there is an additional stresslet induced by the contact force \mathbf{F}^c :

$$S_{ij}^C = \frac{1}{2} a s (1 - A) F_k^c n_k (n_i n_j - \frac{1}{3} \delta_{ij}) + \frac{1}{4} a s (1 - B - 2(y_{11}^h + y_{12}^h)) \times (F_i^c n_j + n_i F_j^c - 2n_i n_j F_k^c n_k), \quad (8)$$

where K , L , M , y_{11}^h and y_{12}^h are also two-sphere hydrodynamic functions (Kim & Karrila, 1991).

The contact forces can also be calculated in terms of two-sphere hydrodynamic functions; they depend additionally on the friction coefficient ν .

2.3 General form of the stress

The most general possible form of the deviatoric part of the stress tensor in a shear flow $\mathbf{u} = \dot{\gamma} y \hat{\mathbf{x}}$ (after taking into account flow symmetries) is:

$$\boldsymbol{\Sigma} = \begin{pmatrix} \Sigma_{xx} & \eta \dot{\gamma} & 0 \\ \eta \dot{\gamma} & \Sigma_{yy} & 0 \\ 0 & 0 & -\Sigma_{xx} - \Sigma_{yy} \end{pmatrix}. \quad (9)$$

The diagonal elements may be expressed in terms of normal stress differences³: by convention, $N_1 = \Sigma_{xx} - \Sigma_{yy}$ and $N_2 = \Sigma_{yy} - \Sigma_{zz} = \Sigma_{xx} + 2\Sigma_{yy}$.

For a dilute suspension, the three rheological functions may in turn be expressed as

$$\eta = \mu \left(1 + \frac{5}{3} c + kc^2 \right) \quad (10)$$

$$N_1 = \mu c^2 \dot{\gamma} \tilde{N}_1 \quad (11)$$

$$N_2 = \mu c^2 \dot{\gamma} \tilde{N}_2. \quad (12)$$

³Wilson and Davis (Wilson and Davis, 2002) erroneously stated that $N_2 \equiv 0$ for a monolayer flow.

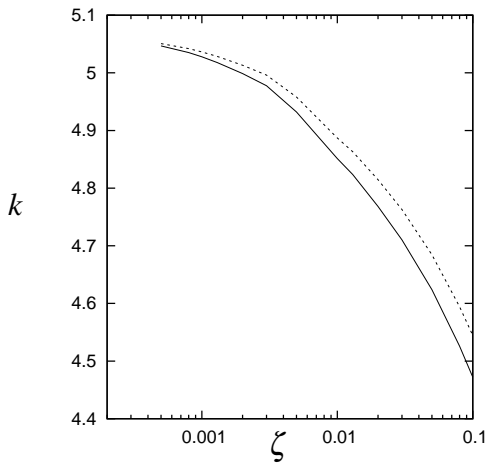


Figure 2: Plot of the $O(c^2)$ contribution to viscosity against roughness height ζ . The lower (solid) curve represents the case of no friction, $\nu = 0$, and the upper (dotted) curve the opposite extreme, $\nu \rightarrow \infty$.

2.4 Results for dilute suspensions

For roughness heights less than the closest approach of a closed orbit, $\zeta < 2.11 \times 10^{-4}$, we cannot calculate the suspension viscosity to order c^2 because of the indeterminacy of \mathcal{P} , as discussed in section 2.1. However, by symmetry the closed orbits do not contribute to the normal stress differences, so N_1 and N_2 may be calculated for all possible values of ζ .

Figure 2 shows the $O(c^2)$ coefficient of viscosity for a range of roughness heights $\zeta > 2.11 \times 10^{-4}$, for the two extreme cases of friction coefficient $\nu = 0$ and $\nu \rightarrow \infty$. There is very little dependence on friction coefficient, but it is clear that increasing roughness decreases the suspension viscosity. This is because the particles are excluded from configurations with very small interparticle gaps, which are precisely those configurations in which lubrication interactions cause strong dissipation.

In figure 3 we show the first normal stress difference N_1 , normalised by $\mu c^2 \dot{\gamma}$, again plotted against roughness height. Roughness is shown to induce a negative value of N_1 , and again we find that the friction coefficient is rather unimportant.

Finally, in figure 4 we show the normalised second normal stress difference $\tilde{N}_2 = N_2 / \mu c^2 \dot{\gamma}$,

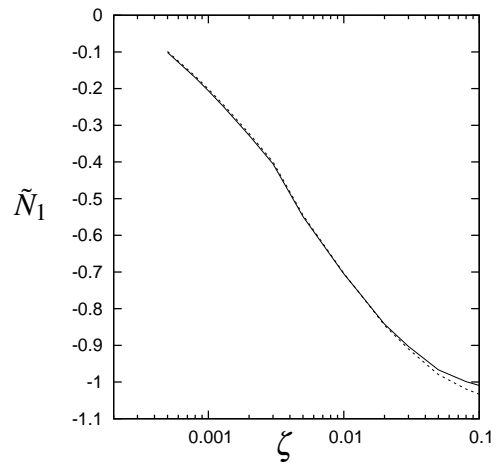


Figure 3: Plot of the normalised first normal stress difference \tilde{N}_1 against the roughness height ζ . The solid curve represents the case of no friction, $\nu = 0$, and the dotted curve the opposite extreme, $\nu \rightarrow \infty$. The curves are almost indistinguishable, indicating that friction is a negligible component of the first normal stress difference.

again plotted against roughness height. Roughness is shown to induce a negative value of N_2 , and again we find that the friction coefficient is rather unimportant. N_2 is smaller in magnitude than N_1 , but only by a factor of around 3–5.

3. Concentrated Suspensions

We are also carrying out simulations of monolayers of rough spheres at higher area fractions. We use the Stokesian Dynamics paradigm, which is essentially a truncated multipole expansion.

For viscosity, our results for concentrated suspensions show two distinct trends. At moderate concentrations, they are in line with our dilute results: roughness reduces viscosity while the coefficient of friction is largely unimportant. Above an area fraction of around 0.4, however, each particle becomes (on average) “close” to more than one neighbour and the dilute theory ceases to be helpful. At around this value, the viscosity begins to increase with roughness height; in addition, the viscosity now rises sharply with increasing coefficient of fric-

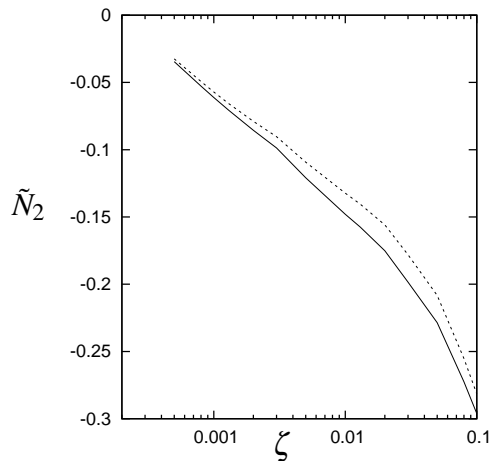


Figure 4: Plot of the normalised first normal stress difference \tilde{N}_2 against the roughness height ζ . The lower (solid) curve represents the case of no friction, $\nu = 0$, and the upper (dotted) curve the opposite extreme, $\nu \rightarrow \infty$.

tion.

The normal stress results are less clear. They depend very strongly on particle configuration and as a result they are strongly oscillatory during a given simulation. It is difficult to be certain of even the sign of the mean normal stress as concentration increases, but our results do suggest the mean is negative for both N_1 and N_2 , in accord with the dilute theory for both two and three dimensional systems (Wilson & Davis, 2000).

Quantitative results for concentrated suspensions will be presented at the meeting.

References

- Arp, P., Mason, S., 1977. The kinetics of flowing dispersions. IX. Doublets of rigid spheres (experimental). *Journal of Colloid and Interface Science* 61, 44–61.
- Batchelor, G., Green, J., 1972. The hydrodynamic interaction of two small freely-moving spheres in a linear flow field. *Journal of Fluid Mechanics* 56, 375–400.
- Brady, J., Bossis, G., 1985. The rheology of concentrated suspensions of spheres in simple shear-flow by numerical-simulation. *Journal of Fluid Mechanics* 155, 105–129.

- De Moss, J., Cahill, K., 2007. Laminar Flow. www.youtube.com/watch?v=p08_KITKP50
- Einstein, A., 1906. Eine neue Bestimmung der Moleküledimensionen. *Annalen Physik* 19, 289–306.
- Einstein, A., 1911. Berichtigung zu meiner Arbeit: “Eine neue Bestimmung der Moleküledimensionen”. *Annalen Physik* 34, 591–592.
- Kim, S., Karrila, S., 1991. *Microhydrodynamics: Principles and selected applications*. Butterworth-Heinemann.
- Wilson, H., Davis, R., 2000. The viscosity of a dilute suspension of rough spheres. *Journal of Fluid Mechanics* 421, 339–367.
- Wilson, H., Davis, R., 2002. Shear stress of a monolayer of rough spheres. *Journal of Fluid Mechanics* 452, 425–441.
- Zeng., S., Kerns, E., Davis, R., 1996. The nature of particle contacts in sedimentation. *Physics of Fluids* 8, 1389–1396.